

## EVALUATION OF TRIBOLOGICAL BEHAVIOR OF TRIBOPAIRS IN WATER HYDRAULIC RADIAL PISTON PUMPS WITH MULTIPLE COATINGS AND LUBRICATION

RAN LI

*Graduate School, China Coal Research Institute, Beijing, China, and  
Beijing Tianma Intelligent Control Technology Co., Ltd., Beijing, China, and  
College of Mechanical and Electronic Engineering, Shandong University of Science and Technology, Qingdao, China*

WENSHU WEI, HAO LIU, XIANGYU GENG, JIANFENG LI, YUEHUA LAI, RONGMING CHEN,  
DONGZE LI, TIANLIANG YU

*Beijing Tianma Intelligent Control Technology Co., Ltd., Beijing, China  
corresponding author Yuehua Lai, e-mail: laiylh@mktm.com.cn*

DALONG WANG

*School of Mechanical Electronic and Information Engineering, China University of Mining and Technology-Beijing,  
Beijing, China*

JIAN YE, SHOUBIN LI, WEI WANG, HUIGANG WU

*Beijing Tianma Intelligent Control Technology Co., Ltd., Beijing, China*

In order to explore the tribological behavior of slipper/eccentric cam tribopairs under different lubrication conditions at power ends of water hydraulic radial piston pumps, friction-wear tests were carried out. It is found that tribopairs under water-based lubrication exhibited better friction-reducing performances than those under water lubrication alone. The average steady-state friction coefficient under water-based lubrication was between 0.17 and 0.23. HMn62-3-3-0.7/17-4PH tribopair using water-based lubrication exhibited the lowest wear rate of  $1.1 \cdot 10^{-12} \text{ mm}^3/\text{N}\cdot\text{m}$ . The findings of this study offer a reference for the identification of potential material pairs for slipper/eccentric cam tribopairs.

*Keywords:* water hydraulic radial piston pump, tribopair, friction-wear, HMn62-3-3-0.7, water-based lubrication

### 1. Introduction

Water hydraulic radial piston pumps (WHRPPs) are widely used in various industrial applications, such as seawater desalination, descaling, and coal mining high hydraulic power (Cotter, 2000; Li *et al.*, 2023, 2024; Zhao *et al.*, 2017). WHRPPs use water or seawater both as a working medium at the liquid ends and as a lubrication medium at the power ends for low-speed and low-pressure applications (Zhang *et al.*, 2017). For high-speed and high-pressure applications, mineral oils are generally used as lubrication media at the power ends of WHRPPs separated by dynamic seals. Damage or failure of dynamic seals results in emulsification of the lubricating oil, which may lead to possible failure of the components, such as slipper/eccentric cam tribopairs at the power ends of the WHRPPs. Significant advancements have been achieved in the design and application of WHRPPs in recent years owing to creation of novel lubricating media that combine exceptional anti-corrosion, anti-wear, and environmentally friendly properties. Therefore, it is important to understand and predict tribological behavior of slipper/eccentric cam tribopairs under different lubrication conditions at the power ends of WHRPPs.

Many studies have been conducted to investigate tribological or lubricating behavior of slipper/swashplate tribopairs in piston pumps under water or seawater lubrication conditions (Nie *et al.*, 2006; Yinshui *et al.*, 2009; Ma *et al.*, 2015; Liang *et al.*, 2023; Nie *et al.*, 2019; Yin *et al.*, 2023; Kou *et al.*, 2022; Wu *et al.*, 2018). Recently, Wei *et al.* (2019) conducted frictional corrosion tests on PEEK/AISI 630 tribopairs on representative slipper/swashplate tribopairs in water hydraulic axial piston pumps under dry, pure water, and seawater lubrication conditions. Wu *et al.* (2020) conducted comparative studies on wear tests for three types of slipper materials, 1Cr18Ni9Ti, ZQSn10-1, and ZQAl10-4-4, and two types of swashplate materials, 38CrMoAl and 45 steel, under dry sliding conditions. Despite the inherent safety and environmental protection of water and seawater lubrication, their applications for long-term and high-efficiency operations are still limited owing to insufficient lubrication performance and low viscosity. Therefore, the addition of functional additives to water-based lubricants, such as water-glycol hydraulic fluids, to improve their tribological and anticorrosive behavior is one of the focal points of research. Zhou *et al.* (2010) studied friction and wear behavior of a-CNx/SiC tribopairs in an ethylene glycol (EG) aqueous solution and found that the concentration of 10 vol.% EG gave the lowest friction coefficient of 0.019. Espinosa *et al.* (2014) showed that an ultra-low minimum friction coefficient of 0.0001 could be obtained for a sapphire/AISI 316 L contact lubricated by a water +1 wt% solution of bis(2-hydroxyethylammonium) succinate.

Several studies have been conducted to develop a novel WHRPP in the field of underground coal mining using environmentally friendly and anticorrosion lubrication (Li *et al.*, 2023, 2024). In this study, friction and wear tests were conducted using pin-on-disk specimens to represent slipper/eccentric cam tribopairs in a WHRPP under various lubrication conditions. Three Cu-based slipper materials and four types of eccentric cam materials/coatings were used. The material and lubrication dependencies were determined and analyzed based on the friction coefficients and wear rates for different pin-on-disk tribopairs. The wear mechanisms of the three Cu-based pin specimens sliding against the 42CrMo4 lower specimens with quench polish quench (QPQ) coatings, which are specialized types of nitrocarburizing case hardening that increases corrosion resistance, were characterized using scanning electron microscopy (SEM) and energy-dispersive X-ray spectroscopy (EDS) analyses. The novel contribution of this study is the identification of potential material pairs for application as slipper/eccentric cam tribopairs in water hydraulic piston pumps under water-based lubrication.

## 2. Experiments

The effects of lubricants on the tribological behavior of slipper/eccentric cam tribopairs in the WHRPPs were investigated by pin-on-disk wear tests using SRV IV friction tester shown in Fig. 1 (frequency = 50 Hz, stroke = 1 mm, test load = 100 N, test duration = 1 h, and temperature = 50°C). The pin-on-disk contact surfaces were wetted with 0.5 mL lubricant before each test.

As shown in Fig. 2, the upper specimens were designed with a diameter of 9.3 mm which tapered to a diameter of 2 mm at the contact surface, and a total height of 10 mm. The diameter and height of the lower specimens were 24.4 mm and 7.9 mm, respectively.

Three Cu-based materials were selected that were potentially suitable for slipper/eccentric cam tribopairs, i.e., HMn62-3-3-0.7, QAL10-5-5 and ZCuPb15Sn8.

The lower specimens consisted of different steel: martensitic precipitation-hardening stainless steel, 17-4PH, alloy steel, 42CrMo4; and nitriding steel 38CrMoAl. A QPQ coating was used to increase the hardness and corrosion resistance of 42CrMo4 and 38CrMoAl lower specimens at a low cost and with low part distortion. The 42CrMo4 lower specimen was also surface-treated with 15 wt.% tungsten carbide (WC)-reinforced Ni-based coating to improve its wear and corrosion resistance when subjected to water-based lubrication (Liu *et al.*, 2001).

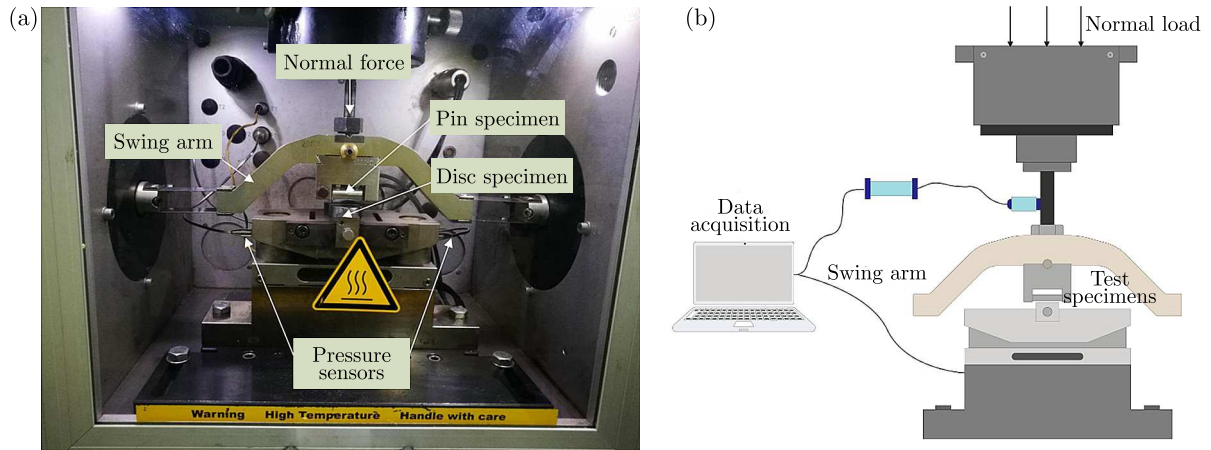


Fig. 1. (a) Test chamber of SRV IV test apparatus; (b) schematic representation of SRV IV test apparatus



Fig. 2. Representation of slipper/eccentric cam pin-on-disc tribopairs

### 3. Results and analysis

#### 3.1. Coefficient of friction

The relationship between the friction coefficients and sliding time of HMn62-3-3-0.7 upper specimens sliding against four types of lower specimens under different lubrication conditions: distilled water, GL-5 85 W-90 oil, and 8 vol.% FF330 water-based lubrication, were determined experimentally, as shown in Fig. 3. The friction coefficients for HMn62-3-3-0.7 sliding against the four types of lower specimens under oil-lubricated conditions reached an approximately steady state, with values in the range of 0.16-0.20. In the water-lubricated condition, the friction coefficients for HMn62-3-3-0.7 sliding against the lower specimens 17-4PH, 42CrMo4-QPQ, and 38CrMoAl-QPQ were in the range of 0.3-0.32, a factor of 1.6 times of those for the oil-lubricated condition. A significant fluctuation in the friction coefficient for the HMn62-3-3-0.7/38CrMoAl-QPQ tribopair, with a peak value of approximately 0.80, indicated that severe wear may occur for each fluctuation. For a 8 vol.% FF330 water-based lubrication, the steady-state friction coefficients for the HMn62-3-3-0.7 sliding against the four types of lower specimens were nearly identical to those under the oil lubricating condition, except for a small amount of fluctuations in the steady states.

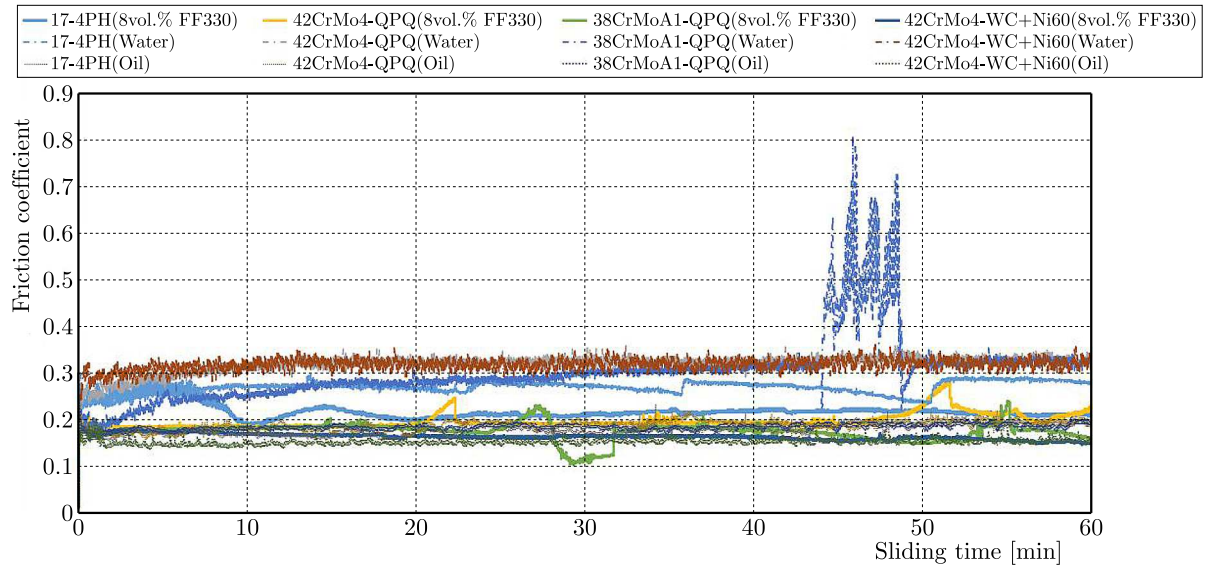


Fig. 3. Variation in friction coefficients of HMn62-3-3-0.7 upper specimens sliding against four types of lower specimens under different lubricating conditions

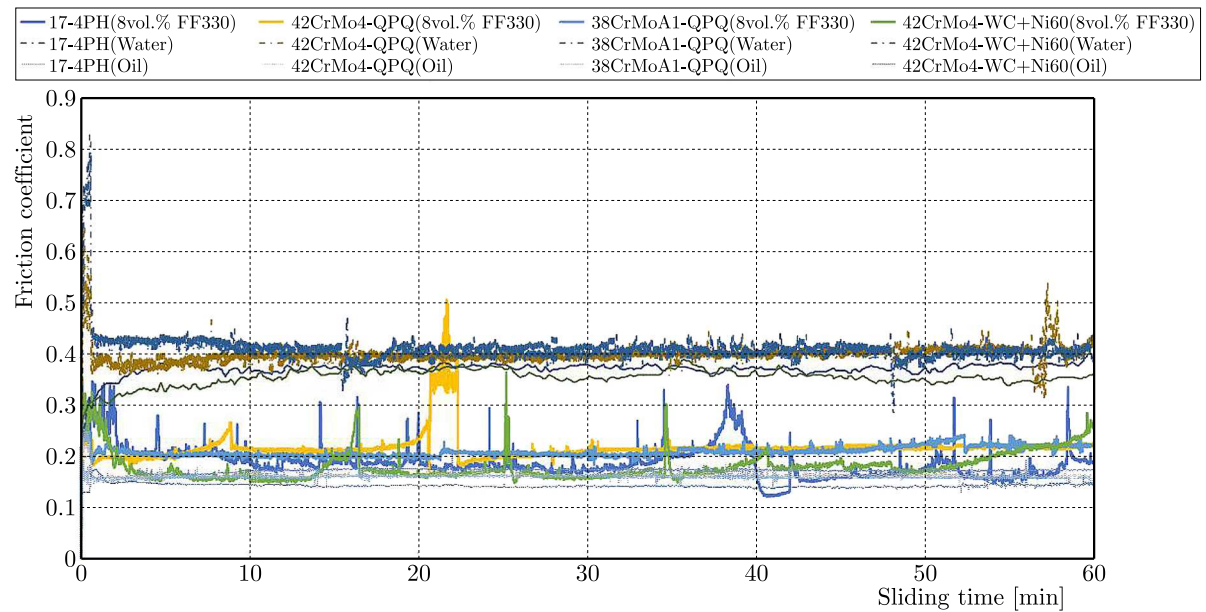


Fig. 4. Variation in friction coefficients of QAL10-5-5 upper specimens sliding against four types of lower specimens under different lubricating conditions

Figure 4 shows the relationship between friction coefficients and sliding time of QAL10-5-5 upper specimens sliding against the four types of lower specimens under three different lubrication conditions. The trend of variation in friction coefficients for QAL10-5-5 upper specimens under oil-lubricated conditions was comparable to that for HMn62-3-3-0.7 upper specimens, which fluctuated greatly in the initial stage, then gradually increased, and finally reached an approximate steady state. The friction coefficients for the oil-lubricated condition are in the range of 0.14-0.17. For HMn62-3-3-0.7 tribopairs in the water-lubricated condition, the steady-state friction coefficients are in the range of 0.35-0.41 for QAL10-5-5 upper specimens against the four types of lower specimens, except for the occurrence of a peak fluctuation of a value of 0.537 for the QAL10-5-5/42CrMo4-QPQ. Numerous fluctuations in the steady-state friction coefficients were observed for the QAL10-5-5/17-4PH, QAL10-5-5/42CrMo4-QPQ, and QAL10-5-

-5/42CrMo4-WC+Ni tribopairs under 8 vol.% FF330 lubrication. The 8 vol.% FF330 lubrication provides good anti-wear behavior for the QAL10-5-5/38CrMoAl-QPQ tribopair, which gives a steady state friction coefficient value of 0.22.

The ZCuPb15Sn8 upper specimens sliding against the four types of lower specimens under water-lubricated conditions showed poor anti-wear behavior, and strong fluctuations occurred during the test, as shown in Fig. 5. Fluctuations in the friction coefficient also occurred during the tests of the 8 vol.% FF330 lubricated tribopairs, especially for the ZCuPb15Sn8/42CrMo4-QPQ tribopair which showed strong fluctuations and a peak friction coefficient of 0.47. Oil lubrication is the only method suitable for preventing the ZCuPb15Sn8 from wear for four types of eccentric cam materials. The steady-state friction coefficients for the ZCuPb15Sn8 upper specimens under oil-lubricated conditions are in the range of 0.16-0.21.

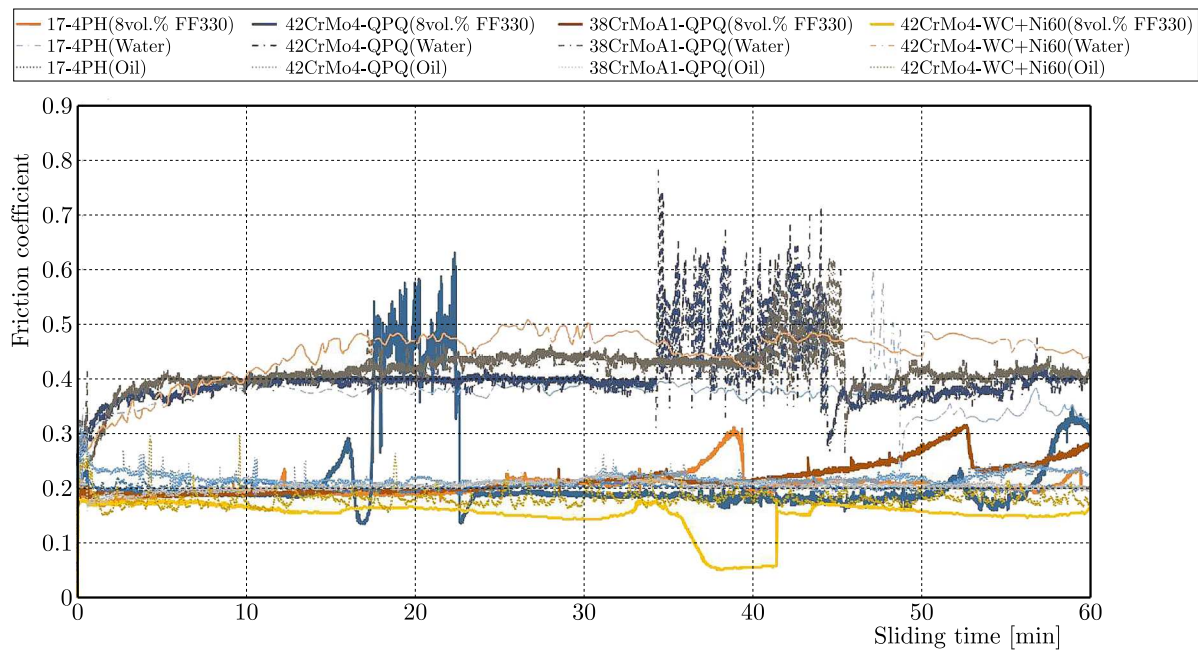


Fig. 5. Variation in friction coefficients of the ZCuPb15Sn8 upper specimens sliding against four types of lower specimens under different lubricating conditions

### 3.2. Wear rate

The wear rate  $W_s$  [ $\text{mm}^3/\text{Nm}$ ] of the materials is given by Eq. (3.1), as proposed in previous studies (Zhang *et al.*, 2015; Yin *et al.*, 2021)

$$W_s = \frac{\Delta m}{\rho N L} \quad (3.1)$$

where  $\rho$  denotes density of the worn material,  $N$  the normal load,  $L$  the total sliding distance, and  $\Delta m$  the wear weight. The weight analysis method based on ISO-14242/2 (2016) was used to measure the wear weights of the upper and lower specimens.

The wear rate comparisons among different tribopairs are shown in Fig. 6. Figures 6a-6c show the wear rates of the HMn62-3-3-0.7, QAL10-5-5, and ZCuPb15Sn8 upper specimens against the four types of lower specimens under oil, water, and 8 vol.% FF380 lubrication, respectively. For the HMn62-3-3-0.7 material, it can be confirmed that lubrication with 8 vol.% FF330 results in lower wear rates for all four types of lower specimens, especially for 38CrMoAl-QPQ which has a much smaller wear rate compared to oil and water lubrication. The QAL10-5-5/17-4PH tribopair showed good anti-wear behavior with all three lubricants, as shown in Fig. 6b. Water



lubrication led to substantially higher wear rates for the alloy steels with different coatings. The 8 vol.% FF330 lubrication for the QAL10-5-5 material produced comparable wear rates compared to the values for oil lubrication. Figure 6c shows that the ZCuPb15Sn8/42CrMo4-WC+Ni tribopair has the lowest wear rates for the three lubricants compared to the wear rates for the ZCuPb15Sn8 upper specimens and the other three steel lower specimens. The ZCuPb15Sn8/42CrMo4-QPQ tribopair exhibited inadequate resistance to wear when lubricated with 8 vol.% FF330. This finding aligns with the friction-coefficient results shown in Fig. 5. With the exception of the ZCuPb15Sn8/42CrMo4-QPQ tribopair, the 8 vol.% FF330 lubrication results in lower wear rates for the other tribopairs compared to the values for oil and water lubrication.

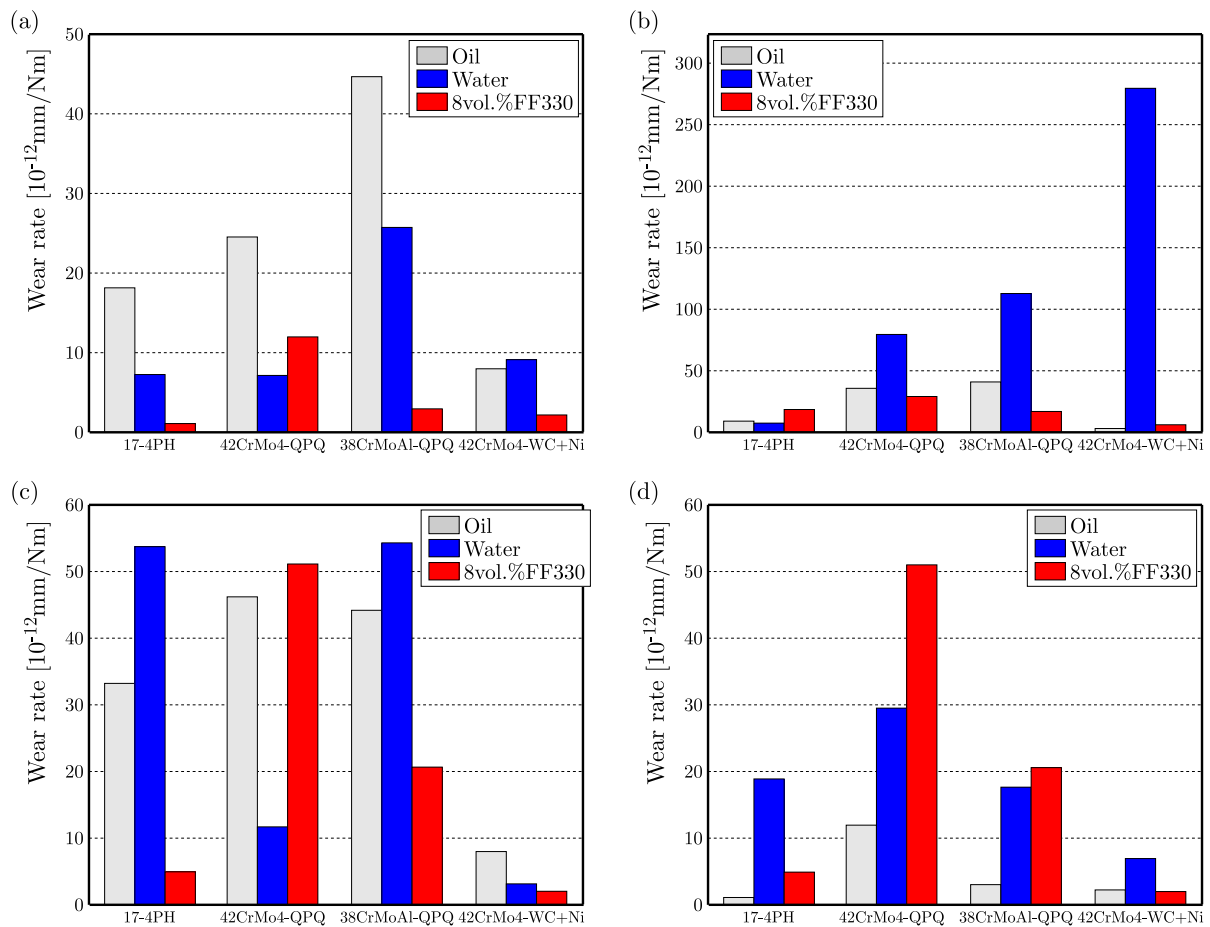


Fig. 6. Wear rate comparisons among different tribopairs: (a) HMn62-3-3-0.7, (b) QAL10-5-5, (c) ZCuPb15Sn8, (d) three Cu-based materials

Figure 6d shows the wear rates of the three Cu-based materials sliding against the four types of eccentric cam materials under 8 vol.% FF330 lubrication. The HMn62-3-3-0.7 material seems to be a good choice for the fabrication of slippers, providing good anti-wear behavior for all four types of lower specimens. Among the four types of lower specimens, the 42CrMo4 alloy steel treated with the spray-welded 15 wt% WC-reinforced Ni-based coating appeared to be the most suitable for making an eccentric cam, which had the lowest wear rates for all three Cu-based upper specimens. The 42CrMo4 alloy steel treated with the QPQ coating should not be used to make an eccentric cam, as it had the highest wear rates for all three Cu-based upper specimens.

### 3.3. SEM morphology analyses

SEM analyses were performed on the worn surfaces of the three Cu-based upper specimens sliding against the 42CrMo4-QPQ lower specimens under oil, water and 8 vol.% FF380 lubrication to characterize the effect of 8 vol.% FF380 lubrication on the wear mechanism of the tribopairs. Figures 7a to 7f show the worn surfaces of the HMn62-3-3-0.7/42CrMo4-QPQ tribopairs under different lubrication conditions.

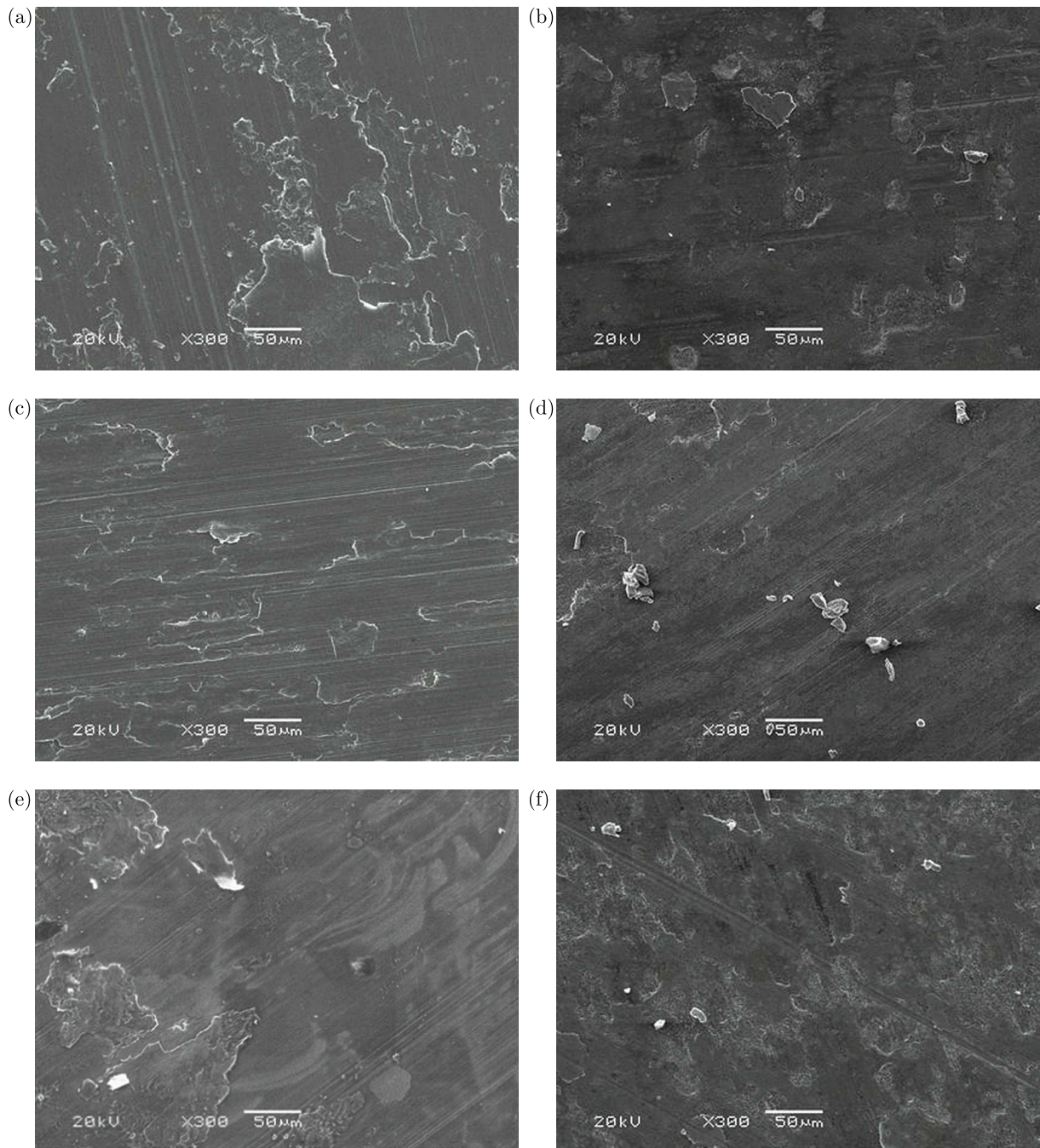


Fig. 7. Worn surfaces of HMn62-3-3-0.7 upper specimens sliding against 42CrMo4-QPQ lower specimens under different lubricating conditions: (a) HMn62-3-3-0.7(oil), (b) 42CrMo4-QPQ(oil), (c) HMn62-3-3-0.7(water), (d) 42CrMo4-QPQ(water), (e) HMn62-3-3-0.7(8vol.% FF330), (f) 42CrMo4-QPQ(8vol.% FF330)

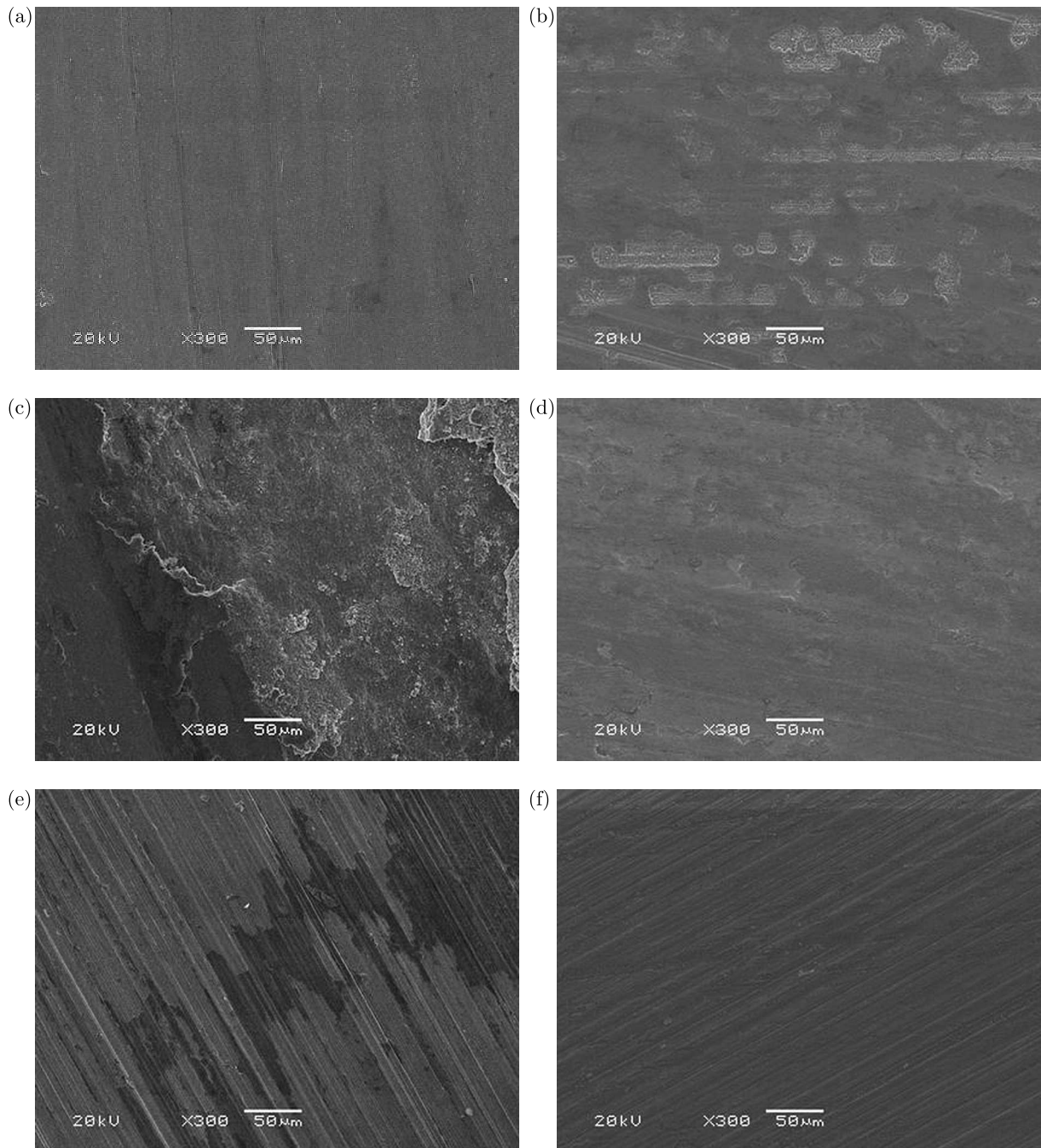


Fig. 8. Worn surfaces of QAL10-5-5 upper specimens sliding against 42CrMo4-QPQ lower specimens under different lubricating conditions: (a) QAL10-5-5(oil), (b) 42CrMo4-QPQ(oil), (c) QAL10-5-5(water), (d) 42CrMo4-QPQ(water), (e) QAL10-5-5(8vol.% FF380), (f) 42CrMo4-QPQ(8vol.% FF380)

As shown in Fig. 7a, wear pits and slight furrows appeared on the worn surface of the HMn62-3-3-0.7 upper specimen when subjected to oil lubrication, which was caused by abrasive wear on the counter surfaces between the HMn62-3-3-0.7 and 42CrMo4-QPQ specimens. There were many grooves on the worn surface of the HMn62-3-3-0.7 upper specimen, indicating that two-body abrasive wear occurred owing to the hard particles embedded in the counter surface of the 42CrMo4-QPQ lower specimen, as shown in Fig. 7c. Plastic deformation occurred around the grooves and oxidation was apparent in these grooves. A large amount of wear debris accumulated on the worn surface of the 42CrMo4-QPQ lower specimen, as shown in Fig. 7d. Adhesive



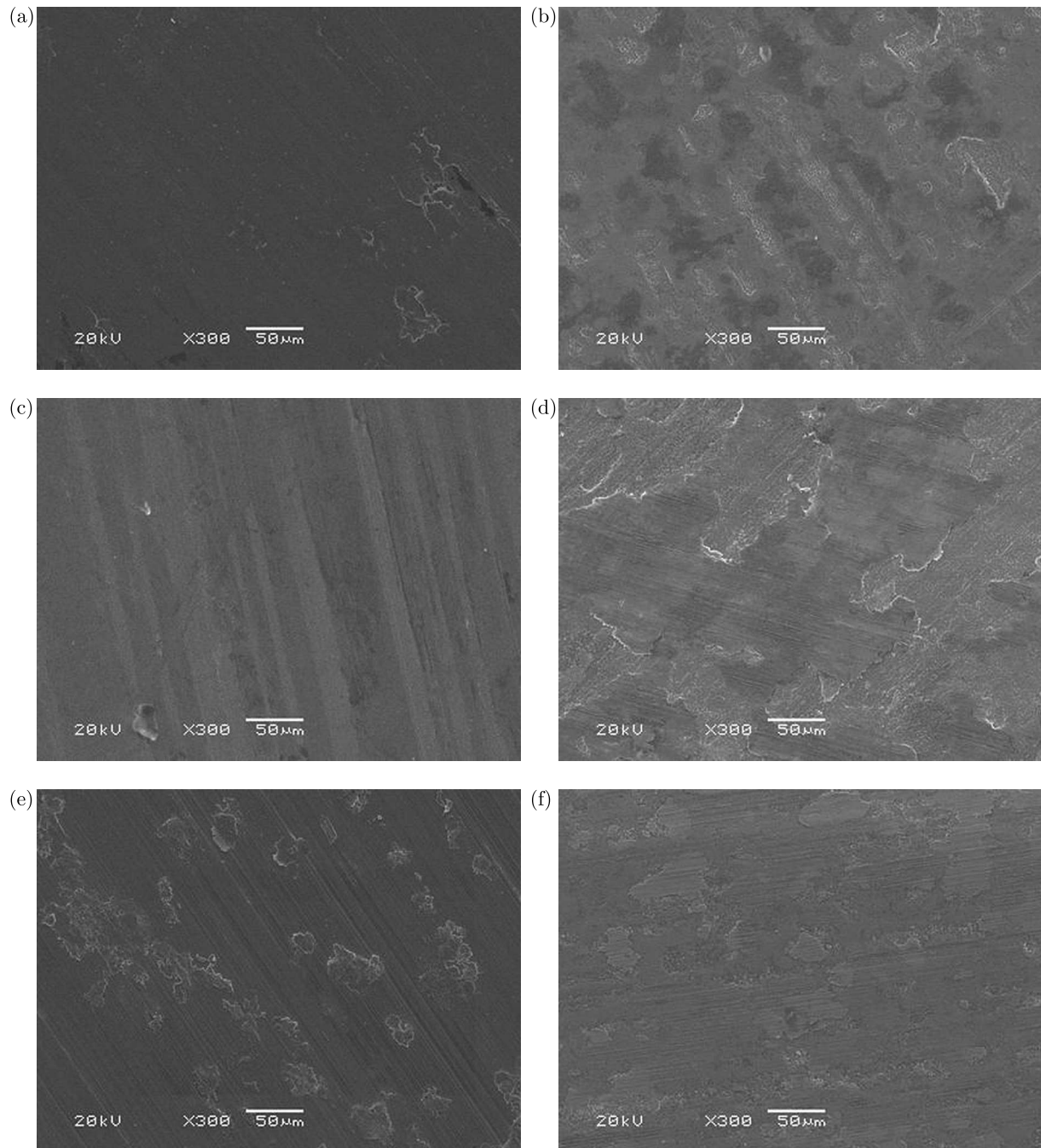


Fig. 9. Worn surfaces of ZCuPb15Sn8 upper specimens sliding against 42CrMo4-QPQ lower specimens under different lubricating conditions: (a) ZCuPb15Sn8(oil), (b) 42CrMo4-QPQ(oil), (c) ZCuPb15Sn8(water), (d) 42CrMo4-QPQ(water), (e) ZCuPb15Sn8(8vol.% FF380), (f) 42CrMo4-QPQ(8vol.% FF380)

wear occurred on the worn surfaces of the HMn62-3-3-0.7 upper specimen and the 42CrMo4-QPQ lower specimen with 8 vol.% FF380 lubrication, as shown in Fig. 7e, which may result in fluctuations in the friction coefficients of the HMn62-3-3-0.7/42CrMo4-QPQ tribopair.

Figures 8a to 8f show the worn surfaces of the QAL10-5-5 upper specimens sliding against the 42CrMo4-QPQ lower specimens under oil, water, and 8 vol.% FF330 lubricating conditions. Figure 8a shows that less wear occurred on the test surface of the QAL10-5-5 upper specimen under oil lubrication. Figure 8c shows that severe adhesive wear occurred on the test surface of the QAL10-5-5 upper specimen under water lubrication. As shown in Fig. 8e, scratches and

oxidation occurred on the worn surfaces of the QAL10-5-5 upper specimen under 8 vol.% FF330 lubrication. A comparison of Fig. 8b, 8d and 8f shows that almost no adherent QAL10-5-5 materials were transferred to the counter surface of the 42CrMo4-QPQ lower specimen under 8 vol.% FF330 lubrication, and the largest amount of QAL10-5-5 debris accumulated on the counter surface of 42CrMo4-QPQ lower specimen when lubricated with water.

The worn surfaces of the ZCuPb15Sn8/42CrMo4-QPQ tribopairs under oil, water and 8 vol.% FF330 lubrication are given in Figs. 9a to 9f. A comparison of Figs. 9a, 9c and 9e shows that water lubrication leads to the best anti-wear behavior, and the 8 vol.% FF330 lubrication provides the worst anti-wear behavior for the ZCuPb15Sn8/42CrMo4-QPQ tribopairs, which shows a good agreement with the wear-rate results for the ZCuPb15Sn8/42CrMo4-QPQ tribopair. Scratching and adhesion occurred on the tested surface of the ZCuPb15Sn8 upper specimen, as shown in Fig. 9e. Adherent ZCuPb15Sn8 materials were found on the counter surfaces of the lower specimens under oil, water and 8 vol.% FF330 lubrication, as shown in Figs. 9b, 9d and 9f.

### 3.4. EDS analyses

EDS analyses, as shown in Figure 10, were performed on the worn areas of the 42CrMo4-QPQ lower specimens sliding against HMn62-3-3-0.7, QAL10-5-5, and ZCuPb15Sn8 lower specimens under 8 vol.% FF330 lubrication. The HMn62-3-3-0.7 debris transferred to the 42CrMo4-QPQ lower specimen can be detected in Fig. 10a. The X-ray intensities of Cu and Zn for FF330 lubrication were much lower than those for water lubrication. In addition, Pb particles were detected in the HMn62-3-3-0.7/42CrMo4-QPQ tribopair under water-lubricated conditions. As shown in Fig. 10b, the QAL10-5-5 debris was transferred to the worn areas of the 42CrMo4-QPQ lower specimen, which contained Cu and Al particles. The X-ray intensities of Cu for the water-lubricated condition are the largest, which is consistent with the wear rate results shown in Fig. 6c. As shown in Fig. 10c, the debris in the worn areas contained Cu and Zn particles transferred from the ZCuPb15Sn8 upper specimens for all three lubrications, with Pb particles detected only for the water-lubricated condition. The X-ray intensities of Cu is highest for the 8 vol.% FF330 lubrication, which shows a good agreement with the wear-rate results given in Fig. 6d.

## 4. Discussion

### 4.1. Material and surface treatment dependence of tribological behavior of tribopairs

Upon examination of the friction coefficient and wear rate data presented in Section 3, it is evident that the upper specimens of HMn62-3-3-0.7 exhibit consistent steady-state friction coefficients and comparatively modest wear rates across nearly all four lower specimen types tested under the three lubrication conditions. Except for the QAL10-5-5/42CrMo4-WC+Ni tribopair under water lubrication, the spray-welded 15 wt% tungsten carbide (WC)-reinforced Ni-based coatings show the lowest wear rates compared with the other tribopairs with different materials, surface treatments and lubrication. The anti-wear behavior of the 38CrMoAl and 42CrMo4 lower specimens with QPQ coatings were worse than that of the 17-4PH and 42CrMo4-WC+Ni lower specimens under the three lubrication conditions.

### 4.2. Effect of lubrication on the tribological behavior of tribopairs

The kinematic viscosity of the 8 vol.% FF330 water-based lubrication at the test temperature, i.e. 50°C, is significantly lower than that of the GL-5 85W-90 oil. The steady-state friction coefficients for the three Cu-based upper specimens sliding against the four types of lower specimens under 8 vol.% FF330 lubrication are close to the tribopairs under GL-5 85W-90 oil-lubricated conditions, except for the presence of some fluctuations. Figure 10 shows that the wear rates

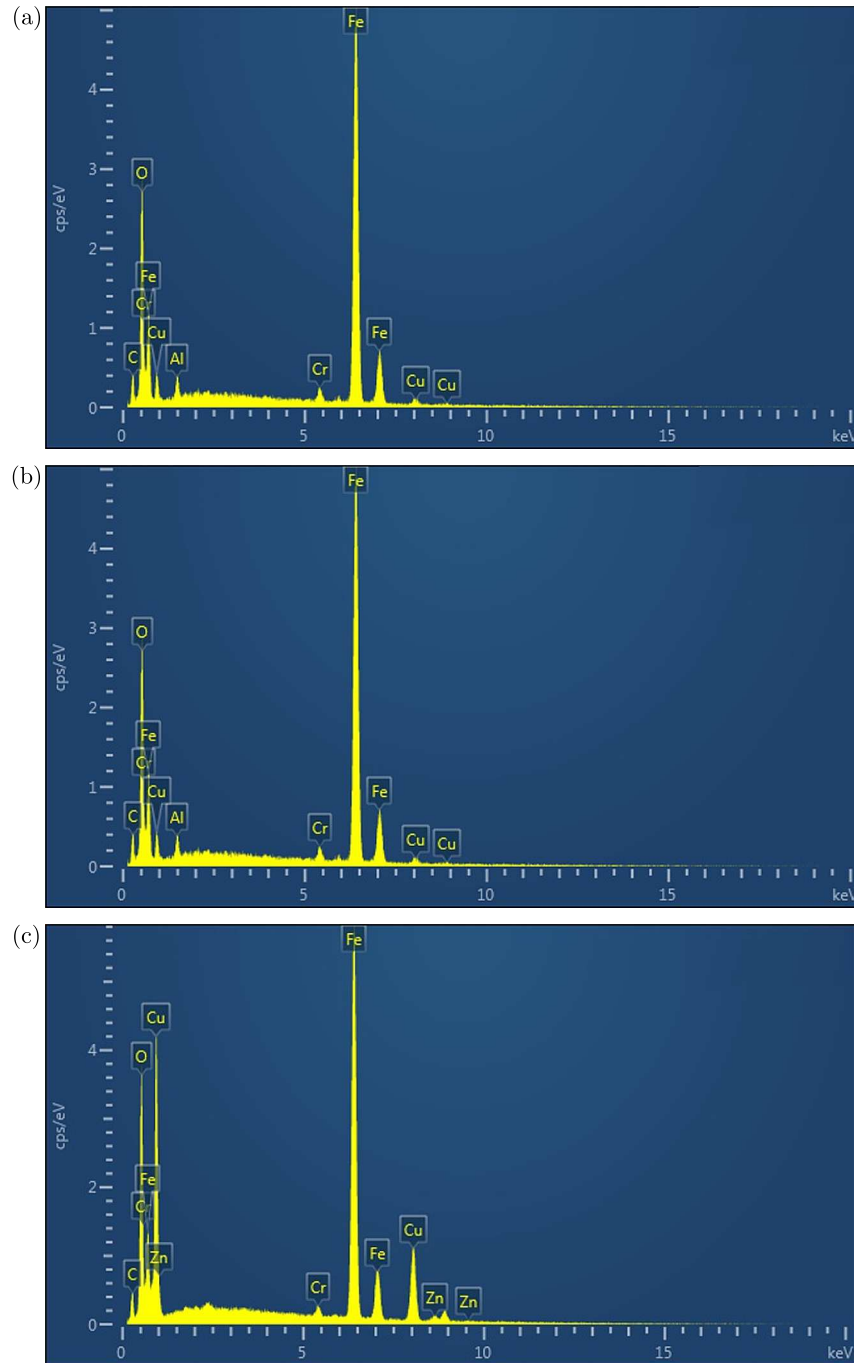


Fig. 10. EDS analyses on worn areas among different tribopairs: (a) 42CrMo4-QPQ against HMn62-3-3-0.7, (b) 42CrMo4-QPQ against QAL10-5-5, (c) 42CrMo4-QPQ against ZCuPb15Sn8

for all tribopairs under 8 vol.% FF330 lubrication are less than  $55 \text{ mm}^3/\text{Nm}$ , much lower than those for the tribopairs under water lubrication. The result of this investigation can be explained by previous studies (Matta *et al.*, 2008; Zhang *et al.*, 2020), which reported that the excellent tribological performance was attributed to the tribochemical transformation of alcohols.

#### 4.3. Effect of initial surface roughness and hardness on tribological behavior of tribopairs

Two surface treatment methods, i.e., the QPQ coating and spray-welded 15 wt% tungsten carbide (WC)-reinforced Ni-based coatings were used to improve the anti-corrosion behavior of representative eccentric cam materials, i.e., 38CrMoAl and 42CrMo4. However, the initial

surface roughness values of the 38CrMoAl and 42CrMo4 lower specimens coated using the quench polishing method were much higher than those of the 42CrMo4 lower specimens coated using the spray welding method. Previous studies have proved that the initial surface roughness values have a significant effect on the “running-in” friction behavior of tribopairs in dry conditions. However, the dominating effect of the initial surface roughness on the friction and wear behavior has not been confirmed under lubricated condition. Dib *et al.* (2020) reported that no large difference in friction coefficients and wear losses could be found for the AISI 304L stainless steel/AISI 52100 alloy steel tribopairs at  $R_a = 0.034 \mu\text{m}$  and  $R_a = 0.72 \mu\text{m}$  when subjected to oil lubrication. Meanwhile, the hardness values for the QPQ coated lower specimens, in the range of 600 HV to 650 HV, are much lower than those for the 15 wt%WC + Ni coated lower specimens having about 950 HV. Therefore, it is likely that the hardness may have an effect on the tribological behavior of the coated specimens.

## 5. Conclusions

In this study, wear tests were performed using pin-on-disk specimens with different coatings and lubrication conditions to evaluate the feasibility of applying water-based lubrication for slipper/eccentric cam tribopairs in WHRPPs. The conclusions are as follows:

- The friction-reducing performance of all tribopairs is found to be superior when lubricated with 8 vol.% FF330 water, which is closely consistent with the test results for friction coefficients under oil lubrication. The steady-state friction coefficients, when lubricated with 8 vol.% FF330 water, exhibit mean values ranging from 0.17 to 0.23.
- In general, tribopairs under 8 vol.% FF330 water-based lubrication showed lower wear rates than those under oil and water lubrication. The lowest wear rate was obtained, i.e.,  $1.1 \cdot 10^{-12} \text{ mm}^3/\text{N}\cdot\text{m}$ , for the HMn62-3-3-0.7 /17-4PH tribopair under 8 vol.% FF330 water-based lubrication.
- The most severe wear was observed on the worn surface of the QAL9-4-4 specimen under water lubrication. Adhesive wear dominated the wear mechanism of QAL9-4-4 sliding against the 42CrMo4-QPQ disc specimens under water lubrication.

This paper provides a concise overview of the impact of material, surface treatment method, lubrication, initial surface roughness, and hardness on the tribological behavior of tribopairs in WHRPPs. We suggest that the tribochemical mechanism of HMn62-3-3-0.7/WC-reinforced Ni-based coated surfaces lubricated with water-ethylene glycol be accounted for in future studies.

### *Acknowledgment*

This research was supported by CCTEG Project (2023-TD-MS015, 2023-TD-QN004) and TMIC Project (2022TM-167M) funding, China.

## References

1. COTTER M., 2000, Rethinking the piston pump – a physicist’s convictions, *World Pumps*, **2000**, 401, 32-33
2. DIB J., HEREÑU S., ALÍ D., PELLEGRINI N., 2020, Influence of load, surface finish and lubrication on friction coefficient of AISI 304 stainless steel, *Journal of Materials Engineering and Performance*, **29**, 5, 2739-2747
3. ESPINOSA T., JIMÉNEZ, M., SANES J., JIMÉNEZ A.E., IGLESIAS M., BERMÚDEZ M.D., 2014, Ultra-low friction with a protic ionic liquid boundary film at the water-lubricated sapphire-stainless steel interface, *Tribology Letters*, **53**, 1-9



4. ISO-14242-2, 2016, Implants for surgery-wear of total hip-joint prostheses – Part 2: Methods of measurement
5. KOU B., LI R., LI Z., HAO R., 2022, Experimental study on the tribological properties of high water-based piston friction pairs with different ceramic materials, *Advances in Mechanical Engineering*, **14**, 8
6. LI R., WEI W., LIU H., GENG X., CUI J., *et al.*, 2024, Design and experimental validation of a valve-distributed water radial piston pump, *Proceedings of the Institution of Mechanical Engineers, Part C: Journal of Mechanical Engineering Science*, **238**, 12, 5488-5497
7. LI R., WEI W., LIU H., GENG X., WANG D., *et al.*, 2023, Tribological behavior of tribo-pairs in water hydraulic radial piston pumps, *Proceedings of the Institution of Mechanical Engineers, Part L: Journal of Materials: Design and Applications*, **237**, 7, 1603-1623
8. LIANG Y., WANG W., ZHANG Z., XING H., WANG C., *et al.*, 2023, Effect of material selection and surface texture on tribological properties of key friction pairs in water hydraulic axial piston pumps: A review, *Lubricants*, **11**, 8, 324
9. LIU S., YU Z., YI D., LI Y., 2001, Chemical pretreatments of the surface of WC-15wt%Co with diamond coatings, *Acta Metallurgica Sinica (English Letters)*, **14**, 2, 143-147
10. MA J., CHEN J., LI J., LI Q., REN C., 2015, Wear analysis of swash plate/slipper pair of axis piston hydraulic pump, *Tribology International*, **90**, 467-472
11. MATTA C., JOLY-POTTUZ L., DE BARROS BOUCHET M.I., MARTIN J.M., KANO M., *et al.*, 2008, Superlubricity and tribochemistry of polyhydric alcohols, *Physical Review B*, **78**, 8, 085436
12. NIE S., LOU F., JI H., YIN F., 2019, Tribological performance of CF-PEEK sliding against 17-4PH stainless steel with various cermet coatings for water hydraulic piston pump application, *Coatings*, **9**, 7, 436
13. NIE S.L., HUANG G.H., LI Y.P., 2006, Tribological study on hydrostatic slipper bearing with annular orifice damper for water hydraulic axial piston motor, *Tribology International*, **39**, 11, 1342-1354
14. WEI L., ZHANG Z., NIE S., WU X., 2019, Direct and indirect corrosion wear performance of AISI 630 steel for the slipper/swashplate pair in a water hydraulic pump, *Proceedings of the Institution of Mechanical Engineers, Part J: Journal of Engineering Tribology*, **233**, 10, 1605-1615
15. WU H., ZHAO L., NI S., HE Y., 2020, Study on friction performance and mechanism of slipper pair under different paired materials in high-pressure axial piston pump, *Friction*, **8**, 5, 957-969
16. WU Z., ZHOU F., WANG Q., 2018, Friction and wear properties of CrSiCN/SiC tribopairs in water lubrication, *Journal of Materials Engineering and Performance*, **27**, 6, 2885-2898
17. YIN F., HE Z., NIE S., JI H., MA Z., 2023, Tribological properties and wear prediction of various ceramic friction pairs under seawater lubrication condition of different medium characteristics using CNN-LSTM method, *Tribology International*, **189**, 108935
18. YIN F., WANG Y., JI H., MA Z., NIE S., 2021, Impact of sliding speed on the tribological behaviors of cermet and steel balls sliding against SiC lubricated with seawater, *Tribology Letters*, **69**, 39
19. YINSHUI L., WU D., HE X., ZHUANGYUN L., 2009, Materials screening of matching pairs in a water hydraulic piston pump, *Industrial Lubrication and Tribology*, **61**, 3, 173-178
20. ZHANG R., CHEN Q., HE Z., XIONG L., 2020, In situ friction-induced amorphous carbon or graphene at sliding interfaces: effect of loads, *Applied Surface Science*, **534**, 146990
21. ZHANG T., ZHANG X., CHEN X., JIA Y., 2017, Numerical investigation on the effect of labyrinth seal configuration on leakage, *MATEC Web of Conferences*, EDP Sciences, **128**, 02013
22. ZHANG Z., NIE S., YUAN S., LIAO W., 2015, Comparative evaluation of tribological characteristics of CF/PEEK and CF/PTFE/graphite filled PEEK sliding against AISI630 steel for seawater hydraulic piston pumps/motors, *Tribology Transactions*, **58**, 6, 1096-1104

23. ZHAO S., GUO T., YU Y., DONG P., LIU C., CHEN W., 2017, Design and experimental studies of a novel double-row radial piston pump, *Proceedings of the Institution of Mechanical Engineers, Part C: Journal of Mechanical Engineering Science*, **231**, 10, 1884-1896
24. ZHOU F., YUE B., WANG Q., WANG X., KOSHI A., KATO K., 2010, Tribological properties of a-CNx coatings sliding against SiC balls in ethylene glycol aqueous solution, *Lubrication Science*, **22**, 6-7, 225-236

*Manuscript received January 11, 2024; accepted for publication October 11, 2024*